A New Operational Method for Estimating Noise in Hyperspectral Images

Article *in* IEEE Geoscience and Remote Sensing Letters · February 2008

DOI: 10.1109/LGRS.2007.909927 · Source: IEEE Xplore

CITATIONS
33

READS
81

5 authors, including:

Bing Zhang
University of Nevada, Las Vegas
646 PUBLICATIONS **10,612** CITATIONS
SEE PROFILE

Xia Zhang
Chinese Academy of Sciences
86 PUBLICATIONS **292** CITATIONS
SEE PROFILE

A New Operational Method for Estimating Noise in Hyperspectral Images

Lian-Ru Gao, Bing Zhang, Xia Zhang, Wen-Juan Zhang, and Qing-Xi Tong

***Abstract*—A new method for estimating noise in hyperspectral images is described in this letter. Our method is based on the general internal regularity of Earth objects and the strong spectral correlation of hyperspectral images. It can be used to automatically estimate noise for both radiance and reflectance images. Unlike other methods discussed in this letter, our method is more reliable and adaptable, which we demonstrate using simulated images with different scene contents. Finally, we successfully applied this new method in estimating noise for Pushbroom Hyperspectral Imager (PHI) data.**

***Index Terms*—Hyperspectral, multiple linear regression, object-seeking algorithm, signal-to-noise ratio (SNR).**

I. Introduction

THE SPECTRAL and spatial de-correlation (SSDC) method [1] has been successfully used for estimating noise in hyperspectral images. The high between-band (spectral) and within-band (spatial) correlations are used to decorrelate the image data via multiple linear regression, and the remaining unexplained residuals are the estimates of noise. Although this method is more reliable for hyperspectral images than other methods based only on the spatial features of images, we found that this method is seriously affected by some kinds of land cover types. In SSDC, the image is divided into rectangular, contiguous, and nonoverlapping blocks. The reason for this is that the spectra of different Earth objects have different relations among the bands, and the small blocks have a high probability of being homogeneous. To reduce the influence of land cover types, and to obtain the best noise estimate, a homogeneous subset of these estimates derived from the small blocks is pooled. However, in some cases, SSDC does not work well for estimating the noise of hyperspectral images, since spectral and spatial correlations of some heterogeneous blocks cannot be removed using simple multiple linear regression.

In this letter, a new method, called homogeneous regions division and spectral de-correlation (HRDSDC), is proposed to automatically estimate signal-to-noise ratios (SNRs) in hyperspectral images. This method is based on the internal regularity of Earth objects and their strong spectral correlations and can be applied to heterogeneous reflectance and radiance images. To demonstrate the stability and the accuracy of this method, we applied it to simulated images—Airborne Visible/Infrared Imaging Spectrometer (AVIRIS) data and Pushbroom Hyperspectral Imager (PHI) data. The results show that our method performed as well as SSDC; in some cases, our method performed even better than SSDC in terms of adaptability and stability.

The noise in imaging spectrometer data sets includes not only periodic sensor noise that can be removed, but also random noise that cannot be removed [2]. The noise estimate in this letter is performed on data sets that have the periodic noise removed. The random noise of the data sets remaining in the optical remote sensing system is generally additive noise, which is independent of the signal [2]–[4]. The signal-plus-noise model described here can be expressed as

$$Z_b(i,j) = S_b(i,j) + N_b(i,j) \tag{1}$$

where Z is the image digital number (DN) with coordinates (i,j) in band b, and $S_b(i,j)$ and $N_b(i,j)$ are the uncorrelated signal and noise components of $Z_b(i,j)$, respectively. All methods discussed in this letter are based on the model expressed in (1).

The remainder of this letter is organized as follows. Section II describes the HRDSDC method. Section III describes the image database used in this study. In Section IV, a comparative performance analysis for HRDSDC and SSDC is presented and discussed. Section V gives a conclusion of this study.

II. Method

In most remote sensing images, the scene primarily consists of many regions arranged in a patchwork manner, where each region corresponds to one class of land cover type. These homogeneous regions are the objects in the scene. When the sampling interval is smaller than the size of an Earth object, the probability of transition from state i to state j is much greater if $j = i$ than if $j \neq i$. Based on this distinctive characteristic of remote sensing images, Kettig and Landgrebe [5] developed an algorithm, called extraction and classification of homogeneous objects (ECHO), for classifying multispectral image data. In his method, the image is divided into many homogeneous regions by first using an object-seeking algorithm. In this algorithm, an image-partitioning transformation is used to delineate the regions of statistically similar pixels before classifying them. Each homogeneous region represents a statistical sample. Then, a sample classifier can be used to classify the objects.

Manuscript received May 22, 2007; revised July 5, 2007. This work was supported by the National Natural Science Foundation of China under Project 40571113.

The authors are with the State Key Laboratory of Remote Sensing Science, Institute of Remote Sensing Application, Chinese Academy of Sciences, Beijing 100101, China (e-mail: lgauss@163.com; zb@irsa.ac.cn; zx_sr@sina.com; zwj1983@gmail.com; tqxi@263.net).

Color versions of one or more of the figures in this paper are available online at http://ieeexplore.ieee.org.

Digital Object Identifier 10.1109/LGRS.2007.909927

However, the processing speed of ECHO is a little higher for the homogeneous regions division. Geng *et al.* [6] developed a new classification algorithm for hyperspectral images based on the internal regularity of Earth objects. His object-seeking algorithm is quite simple and can be used to divide the hyperspectral image into many homogeneous regions. Each region contains one Earth object, and each spectrum of the same region has a similar between-bands correlations.

The new method described in this letter (HRDSDC) greatly employs the internal regularity of Earth objects and the strong spectral correlations of hyperspectral images. We adopt the object-seeking algorithm developed by Geng *et al.* [6] to produce homogeneous regions. The between-band correlations of each region are removed using multiple linear regression. The standard deviation (SD) of the remaining residuals of each region is calculated as the noise estimate of that region. The mean value of these estimates is used as the best estimate of the band noise. HRDSDC is implemented in three steps:

1) dividing the homogeneous regions by an object-seeking algorithm based on the internal regularity of Earth objects;
2) computing estimates of the noise SDs in each region using multiple linear regression;
3) achieving the best estimate of the noise SD of the image.

A. Homogeneous Regions Division

In most cases, when the Earth objects are larger than the size of a pixel, their distribution in remote sensing images is considered to be continuous. This means that if a pixel belongs to class A, the pixels surrounding it are also likely to be class A. This characteristic is adopted to divide the image into small homogeneous regions. To clearly explain this image-partitioning algorithm, we take a hyperspectral image that is m rows high and n pixels wide as an example. In this image, $\mathbf{D}(i,j)$ describes the spectrum at position (i,j), and S_{ij} describes the label of the region in which the pixel (i,j) belongs, where $1 \le i \le m$, and $1 \le j \le n$. $F(x,y)$ denotes the degree of similarity of the adjacent pixels x and y. The decision rule is that y belongs to the same region as x if $F(x,y) \le c$ (or $F(x,y) \ge c$), otherwise, y is a new region; here, c is a prespecified threshold. The pixel in the upper left corner of the image is labeled region 1. The general processing sequence of the image partitioning is from left to right and from top to bottom. Fig. 1 describes the process of image partitioning. There are five possibilities in this processing, which are specified below as a), b), c), d), and e), and are illustrated in Fig. 1.

a) The pixel is in the upper left corner of the image: $S_{11} = 1$.
b) The pixels are in the first row of the image $(i = 1)$: if $F(\mathbf{D}_{1,j-1}, \mathbf{D}_{1,j}) \le c$, then $S_{1,j} = S_{1,j-1}$, otherwise, $S_{1,j} = S_{1,j-1} + 1$, where $j = 2, 3, \ldots, n$.
c) The pixels are in the first column, and not in the first row of the image $(j = 1$ and $i \ne 1)$: if $t \le c$ and $F(\mathbf{D}_{i,1}, \mathbf{D}_{i-1,\mathrm{q}}) = t$, then $S_{i,1} = S_{i-1,q}$, otherwise, $S_{i,1} = \max(S) + 1$, where $t = \min(F(\mathbf{D}_{i,1}, \mathbf{D}_{i-1,1}), F(\mathbf{D}_{i,1}, \mathbf{D}_{i-1,2}))$, $i = 2, 3, \ldots, m$.

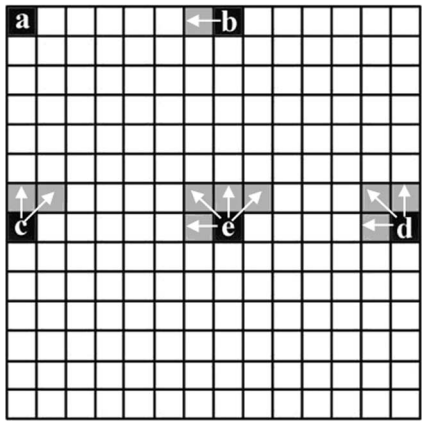

Fig. 1. Map of the object-seeking algorithm.

d) The pixels are in the last column, and not in the first row of the image $(j = n$ and $i \ne 1)$: if $t \le c$ and $F(\mathbf{D}_{i,n}, \mathbf{D}_{p,q}) = t$, then $S_{i,n} = S_{p,q}$, otherwise, $S_{i,n} = \max(S) + 1$, where $t = \min(F(\mathbf{D}_{\mathrm{i},n}, \mathbf{D}_{i,n-1}), F(\mathbf{D}_{i,n}, \mathbf{D}_{i-1,n-1}), F(\mathbf{D}_{i,n}, \mathbf{D}_{i-1,n}))$, $i = 2, 3, \ldots, m$.
e) The pixels are not at the aforementioned positions $(i \ne 1$, $j \ne 1$, and $j \ne n)$: if $t \le c$ and $F(\mathbf{D}_{i,j}, \mathbf{D}_{p,q}) = t$, then $S_{i,j} = S_{p,q}$, otherwise, $S_{i,j} = \max(S) + 1$, where $t = \min(F(\mathbf{D}_{i,j}, \mathbf{D}_{i,j-1}), F(\mathbf{D}_{i,j}, \mathbf{D}_{i-1,j-1}), F(\mathbf{D}_{i,j}, \mathbf{D}_{i-1,j}), F(\mathbf{D}_{i,j}, \mathbf{D}_{i-1,j+1}))$, $i = 2, 3, \ldots, m$ and $j = 2, 3, \ldots, n-1$.

B. Estimating the Noise SD

After the image data are divided into many homogeneous nonoverlapping regions, the spectral correlation of each region in the data is removed using multiple linear regression. The SD of the residuals obtained by using this procedure is used to estimate band noise. The homogeneous regions obtained in this letter are polygonal, and all of the pixels in the same region have similar correlations between the bands. Therefore, unlike SSDC, in which spatial correlation is also used, we only use the data in bands $k-1$, k, and $k+1$ to estimate the noise in band k. We assume that a region contains h pixels, and $x_{i,k}$ is the pixel in band k at the position i of the region $(1 \le i \le h)$. The predicted value for pixel $x_{i,k}(\hat{x}_{i,k})$ is computed as follows:

$$\hat{x}_{i,k} = a x_{i,k-1} + b x_{i,k+1} + c \tag{2}$$

where a, b, and c are the coefficients computed using multiple linear regression models. The residual $r_{i,k}$ is computed as

$$r_{i,k} = x_{i,k} - \hat{x}_{i,k}. \tag{3}$$

For this region, the unbiased SD, namely, σ_x of the residuals is used as the estimate of the noise

$$\sigma_x = \sqrt{(n-3)^{-1} \sum_{i=1}^{n} r_{i,k}^2} \tag{4}$$

where $n-3$ means that three parameters are used in the multiple linear regression model and that the degree of freedom is reduced from n to $n-3$.

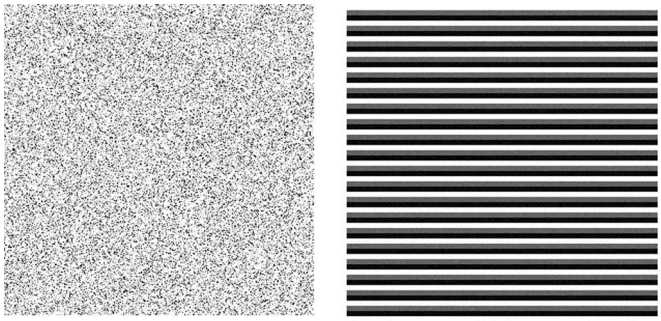

Fig. 2. Two simulated images for noise estimates. (a) Without texture features. (b) With a horizontal strip.

The spectral angle distance (SAD) is a widely used spectral similarity measure for hyperspectral images. It is related to the shape of the spectrum and is insensitive to illumination [12]. Thus, in this letter, SAD is used as $F(x, y)$ to compute the degree of similarity of adjacent pixels, and the prespecified threshold c is 0.1 rad, which is the default threshold used in Environment for Visualizing Images (ENVI) software for hyperspectral image classification [7].

To overcome the influence of parameter selections, some empirical settings are given below. In HRDSDC, the regions with more than 50 pixels are used to estimate noise SD using multiple linear regression. The best noise estimate of the entire image is the mean value of the SDs of all regions with the same weight.

III. Experimental Data Sets

To illustrate the influences of the land cover types, we use SSDC and HRDSDC to estimate the noise in two simulated hyperspectral images with simple texture features. HRDSDC is also used to estimate noise of actual hyperspectral images with different land cover contents. To compare the result conveniently, all images used in this letter are of the same size—300 $\times$ 300 pixels.

A. Simulated Images With Simple Texture Features

Three spectra are used in the image simulation. These spectra, representing three different Earth objects, are extracted from the AVIRIS reflectance image. They are man-made materials, vegetation, and soil, which are labeled as A, B, and C, respectively. The first simulated image with no texture features shown in Fig. 2(a) is created using the spectrum of A. The second simulated image with a horizontal strip pattern shown in Fig. 2(b) is created using spectra of A, B, and C. The strip is five pixels wide and alternates in the order of B, C, and A. The noise SDs of these two simulated images are approximately 2% of the mean DN of each band.

B. PHI Reflectance Images

PHI was developed by the Shanghai Institute of Technical Physics, China, in 1995 [8]. It has been widely used to acquire hyperspectral images from aircraft platforms. The technical characteristics of PHI are shown in Table I.

TABLE I
Technical Characteristics of PHI

Parameters	Performance
Image acquisition mode	CCD push-broom
FOV	0.36 radian
IFOV	1.0 milliradian
Band number	224
Spectral range	VIS-NIR (400~850nm)
Spectral resolution	<5nm
Spectral intervals	1.86nm
Samples	367 pixels/line

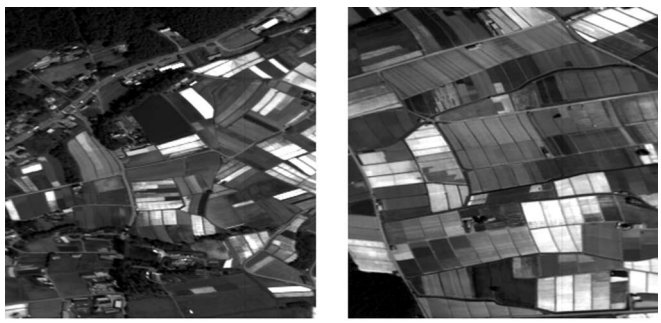

Fig. 3. Band 20 (centered at 561.5 nm) of PHI reflectance images. Panel (a) contains irregular urban areas and regular farmlands. Panel (b) Covered by regular farmlands.

The two PHI images used here contain 80 bands and were acquired at Nagano, Japan, in 2000 (Fig. 3).

IV. Results

The review and assessment of noise estimate methods by Gao [4] and Roger and Arnold [1] show that SSDC is more reliable for estimating noise in hyperspectral images than the homogeneous area (HA) [2], geostatistical (GS) [9], and local means and local SDs (LMLSD) [4] methods. This has also been demonstrated in experiments with data sets from the Operational Modular Imaging Spectrometer (OMIS), which is another airborne imaging spectrometer developed by the Shanghai Institute of Technical Physics [10], [11]. Thus, the noise estimates for experimental images using SSDC and HRDSDC were compared in this study.

We implemented SSDC with a block size of 15 $\times$ 15 pixels. In SSDC, to select a reasonably homogeneous subset of the SDs, we sorted them by size and deleted the top and bottom 10%, leaving approximately 320 values to calculate the best estimate.

A. Illustrate the Influences of the Land Cover Types Using Simulated Images With Simple Texture Features

The results of noise estimation for the simulated images with SSDC are shown in Fig. 4(a). When the entire image is

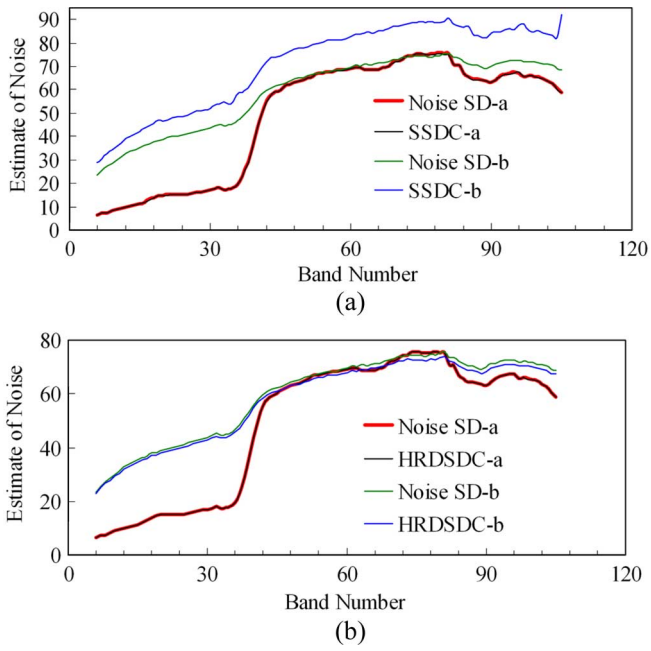

Fig. 4. Noise estimates for simulated images shown in Fig. 2 using SSDC and HRDSDC. Noise SD-a and Noise SD-b are the simulated noise SDs. In (a), SSDC-a and SSDC-b are the noise SDs calculated using SSDC. In (b), HRDSDC-a and HRDSDC-b are the noise SDs calculated using HRDSDC.

homogeneous, the noise SDs estimated by SSDC are almost the same as the simulated noise SDs. However, when every small block in the image is heterogeneous and, consequently, the homogeneous subset selection of SDs cannot eliminate the influence of land cover types, estimates of the noise SDs using SSDC are distinctly different from the simulated noise SDs. Estimated results of the noise by HRDSDC are shown in Fig. 4(b). Compared with the real noise SDs, the mean difference of noise estimates computed by SSDC are -0.086 and 11.662, whereas the mean difference of noise estimates computed by HRDSDC are lower: down to $-4.260\times^{-5}$ and -1.307. HRDSDC provides better noise estimates for the simulated images than SSDC.

From this test, we can see that SSDC is not suitable to remove correlations of heterogeneous blocks using a simple regression model with only four coefficients. This test showed another disadvantage of SSDC, i.e., when the entire image is homogeneous, the block division process still needs to be performed. This means that SSDC cannot adapt to the homogeneity of the image. In HRDSDC, the image is divided into many homogeneous regions, each divided region only contains one Earth object, and the residuals are more approximate to the real noise than those of SSDC.

B. Applying HRDSDC to Estimate Noise in PHI Reflectance Images

HRDSDC is also applied to estimate noise in PHI reflectance images. The results are shown in Fig. 5. These two PHI images are cut from the same image acquired in an aerial experiment. Their qualities should, thus, be similar. However, SSDC obtained very different noise estimates in the 712–731 nm spectral range. This is because there are very heterogeneous land covers

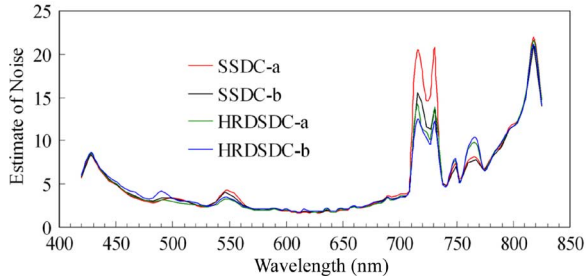

Fig. 5. Estimates of the noise for PHI reflectance images using HRDSDC and SSDC, where -a and -b correspond to (a) and (b), as shown in Fig. 3.

in Fig. 3(a), and the main cover type, urban areas, and vegetation have different spectral correlations in that spectral range, where it is exactly the so-called "Red Edge" of the vegetation [13]. This situation does not occur when we use HRDSDC to estimate noise. Thus, the performance of SSDC may also be affected by some land cover types. In contrast, HRDSDC demonstrates better reliability and adaptive abilities with all the images used in this study.

V. Conclusion

Hyperspectral images always have low spatial resolution and high spectral resolution. Therefore, in hyperspectral images, the between-band correlations are higher than the spatial correlation. HRDSDC is based on high spectral correlations like SSDC and use the algorithm described in [6] to get the homogeneous regions. Unlike SSDC, HRDSDC only makes use of similar spectral correlations of the same Earth object and does not adopt spatial characteristics as an important parameter in noise estimation. Therefore, HRDSDC is less sensitive to spatial features.

In this study, 22 AVIRIS images, except the PHI images displayed in Fig. 3, were also used to test HRDSDC, and our results show that HRDSDC works well for hyperspectral images with very different land cover types. We also demonstrated that HRDSDC works well for both radiance and reflectance images when the SNR of the image is higher than 5 : 1 (common for most imaging spectrometer data sets). HRDSDC is more reliable and adaptable for hyperspectral images than SSDC.

In this letter, we only consider SNR as a criterion for evaluating the image quality and do not take interference into account. The interference is considered as a separate unknown source in addition to signals and noise. It has been shown that the effect of interference is more serious than noise in hyperspectral images [14], [15]. Therefore, signal-to-interference-plus-noise ratio is a better criterion to evaluate the image quality than SNR [16]. In future works, we intend to calculate the effect of interference and develop a new method for estimating the interference in hyperspectral images.

Our new method is more robust for hyperspectral images than other methods discussed in this letter. It can be used to evaluate the capabilities of the remote sensing system. It can also be used to evaluate the hyperspectral image quality in data processing and applications, such as image restoration, classification, target detection, spectral unmixing, and quantitative derivation.

ACKNOWLEDGMENT

The authors would like to thank Dr. Roger and Dr. Geng for discussions and comments on this letter, Jack Teng for some good advice on this letter, and the Jet Propulsion Laboratory for generously providing the AVIRIS data.

REFERENCES

[1] R. E. Roger and J. F. Arnold, "Reliably estimating the noise in AVIRIS hyperspectral images," *Int. J. Remote Sens.*, vol. 17, no. 10, pp. 1951–1962, 1996.

[2] F. D. Van Der Meer and S. M. Dejong, *Imaging Spectrometry: Basic Principles and Prospective Applications*. Dordrecht, The Netherlands: Kluwer, 2001, pp. 35–38.

[3] B. R. Corner, R. M. Narayanan, and S. E. Reichenbach, "Noise estimation in remote sensing imagery using data masking," *Int. J. Remote Sens.*, vol. 24, no. 4, pp. 689–702, Feb. 2003.

[4] B.-C. Gao, "An operational method for estimating signal to noise ratios from data acquired with imaging spectrometers," *Remote Sens. Environ.*, vol. 43, no. 1, pp. 23–33, Jan. 1993.

[5] R. L. Kettig and D. A. Landgrebe, "Classification of multispectral image data by extraction and classification of homogeneous objects," *IEEE Trans. Geosci. Electron.*, vol. GE-14, no. 1, pp. 19–26, Jan. 1976.

[6] X.-R. Geng, X. Zhang, Z.-C. Chen, B. Zhang, L.-F. Zheng, and Q.-X. Tong, "Classification algorithm based on spatial continuity for hyperspectral image," *J. Infrared Millim. Waves*, vol. 23, no. 4, pp. 299–302, 2004.

[7] P. Boccardo, E. Borgogno Mondino, and F. Giulio Tonolo, "Applications based on orthocorrected high resolution and hyperspectral images," *Int. Arch. Photogramm. Remote Sens. Spat. Inf. Sci.*, vol. 35, no. 7, pp. 1067–1072, 2004.

[8] S. Hui, Y. Q. Xue, and J. Y. Wang, "Development of Chinese Pushbroom Hyperspectral Imager (PHI)," *Proc. SPIE—Int. Soc. Opt. Eng.*, vol. 3505, pp. 108–115, 1998.

[9] P. J. Curran and J. L. Dungan, "Estimation of signal-to-noise: A new procedure applied to AVIRIS data," *IEEE Trans. Geosci. Remote Sens.*, vol. 27, no. 5, pp. 620–628, Sep. 1989.

[10] Q. L. Chen and Y. Q. Xue, "Estimation of signal-noise-ratio from data acquired with OMIS," *J. Remote Sens. (Chinese)*, vol. 4, no. 4, pp. 284–289, 2000.

[11] Q. S. Jiang and J. Y. Wang, "Study on signal-to-noise ratio estimation and compression method of Operational Modular Imaging Spectrometer multi-spectral images," *Acta Opt. Sin. (Chinese)*, vol. 23, no. 11, pp. 1335–1340, 2003.

[12] N. Keshava and J. F. Mustard, "Spectral unmixing," *IEEE Signal Process. Mag.*, vol. 19, no. 1, pp. 44–57, Jan. 2002.

[13] R. Pu, P. Gong, G. S. Biging, and M. R. Larrieuc, "Extraction of red edge optical parameters from Hyperion data for estimation of forest leaf area index," *IEEE Trans. Geosci. Remote Sens.*, vol. 41, no. 4, pp. 916–921, Apr. 2003.

[14] C.-I Chang, T.-L. Sun, and M. L. G. Althouse, "An unsupervised interference rejection approach to target detection and classification for hyperspectral imagery," *Opt. Eng.*, vol. 37, no. 3, pp. 735–743, Mar. 1998.

[15] C.-I Chang and C. Brumbley, "An orthogonalization target signature space projection approach to image classification in unknown background," in *Proc. 31st Conf. Inf. Sci. Syst.*, 1997, pp. 174–178.

[16] C.-I Chang and Q. Du, "Interference and noise-adjusted principal components analysis," *IEEE Trans. Geosci. Remote Sens.*, vol. 37, no. 5, pp. 2387–2396, Sep. 1999.